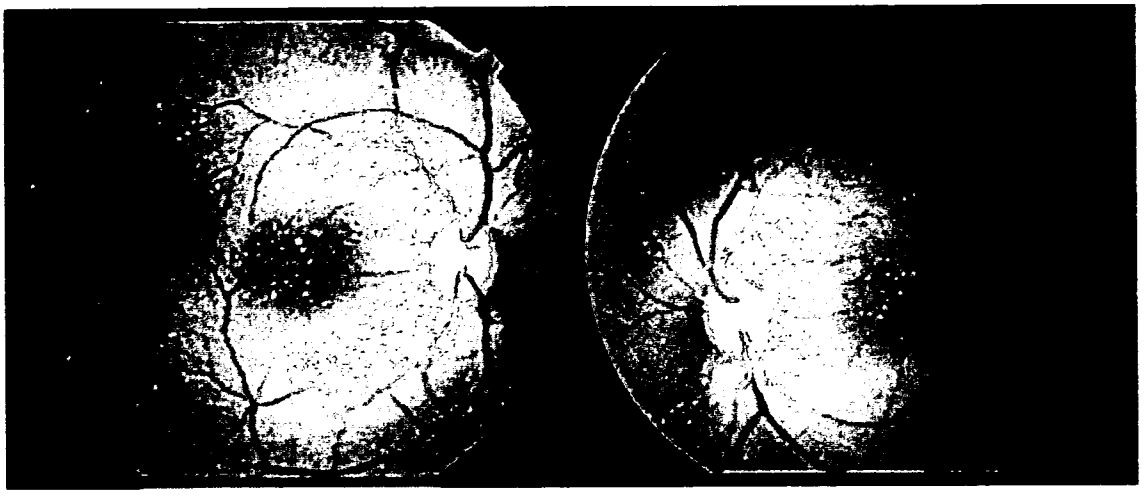

Fig. 1. Fundus photograph of both eyes of Suzuki Monkey showing accumulation of drusen (white spot) around the macular region.

macular degeneration sporadically found in older monkeys and also with human drusen (Umeda, Ayyagari, Allikmets, Suzuki, Karoukis, Ambasudhan, Zernant, Okamoto, Ono, Terao, Mizota, Yoshikawa, Tanaka, and Iwata 2005; Umeda, Suzuki, Okamoto, Ono, Mizota, Terao, Yoshikawa, Tanaka, and Iwata 2005; Ambati, Anand, Fernandez, Sakurai, Lynn, Kuziel, Rollins, and Ambati 2003). These observations have shown that the Suzuki Monkeys produce drusen that are biochemically similar to those in human AMD patients, but the development of the drusen occurs at an accelerated rate. More than 240 loci are being investigated to try to identify the disease causing gene and to understand the biological pathways leading to complement activation. Simultaneously, we have been studying a colony of aged monkeys which develop drusen after 15 years of birth.

Drusen components of these sporadically found affected monkeys were compared with human and Suzuki Monkeys by classical immunohistochemical techniques and by proteome analysis using mass spectrometer. Significant finding was that drusen contained protein molecules that mediate inflammatory and immune processes. These include immunoglobulins, components of complement pathway, and modulators for complement activation (e.g., vitronectin, clusterin, membrane cofactor protein, and complement receptor-1), molecules involved in the acute-phase response to inflammation (e.g., amyloid P component, α1-antitrypsin, and apolipoprotein E), major histocompatibility complex class II antigens, and HLA-DR antigens (Umeda et al. 2005). Cellular components have also been identified in drusen, including RPE debris, lipofuscin, and melanin, as well as processes of choroidal dendritic cells, which are felt to contribute to the inflammatory response. In addition to immune components, a number of other proteins were found in drusen. These appear to be vitronectin, clusterin, TIMP-3, serum amyloid P component, apolipoprotein E, IgG, Factor X, crystallins, EEFMP1, and amyloid-beta. The presence of immunoreactive proteins and oxidative modified proteins implicate both oxidation and immune functions in the pathogenesis of AMD.

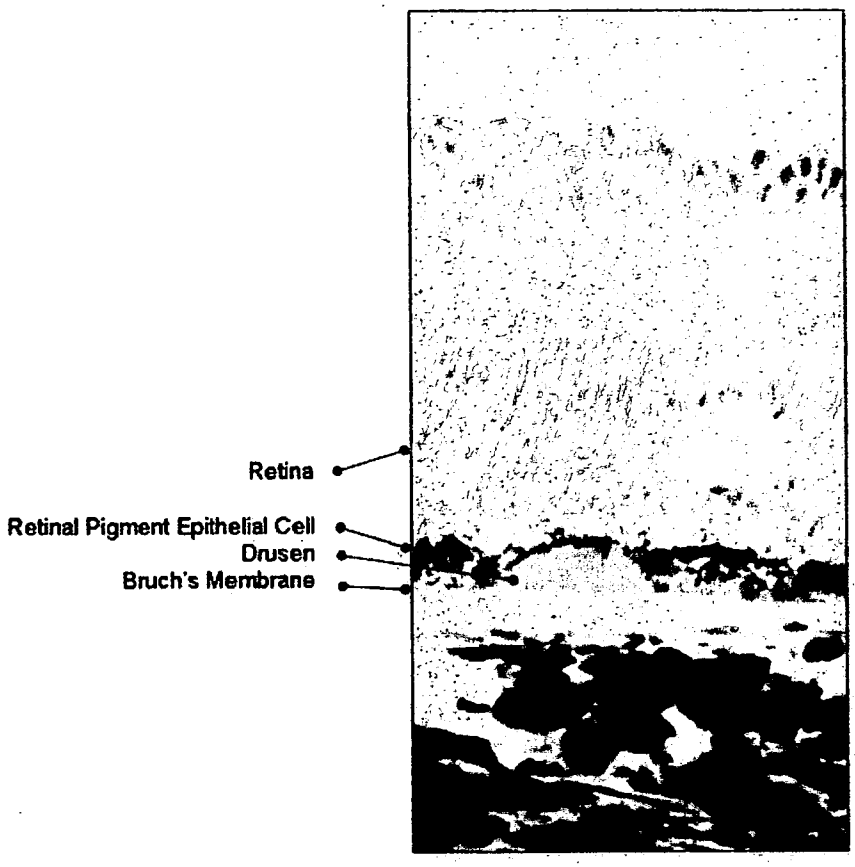

Fig. 2. Retinal histological section of affected Suzuki Monkey showing the accumulation of drusen between the retinal pigment epithelium and Bruch's membrane.

The eyes of monkey are structurally similar to human eyes which make them extremely valuable for AMD studies. However, there are limitations in using this species over other laboratory animals. Monkeys have a relatively longer life span, have a longer gestation period, have a lower birth numbers resulting in a slower expansion of the pedigree, more difficult to genetically manipulate, and the maintenance cost is high. In the other laboratory animals, the differences in the eye structure, lack of a fovea, and a low cone/rod ratio compared to humans have been considered to be a disadvantage for using them as AMD models. However, they are easier to manipulate genetically and easier and less expensive to maintain. This has made the development of a mouse model of AMD very attractive, and a number of mouse AMD models have been reported recently.

6 Mouse Model for AMD

The mouse model described by Ambati et al is deficient either in monocyte chemoattractant protein-1 or its cognate C-C chemokine receptor-2. These mice were found to develop the cardinal features of AMD including accumulation of lipofuscin

in drusen beneath the RPE, photoreceptor atrophy, and CNV (Ambati et al. 2003). An impairment of macrophage recruitment allowed the accumulation of C5a and IgG, which leads to the production of vascular endothelial growth factor by the RPE cells and the development of CNVs. Another mouse model that has three known AMD risk factors: age, high fat cholesterol rich diet, and expression of human apolipoprotein E (apoE2, apoE3, apoE4) has been developed (Malek, Johnson, Mace, Saloupis, Schmechel, Rickman, Toth, Sullivan, and Bowes Rickman 2005). ApoE4-deficient mice are severely affected showing diffuse subretinal pigment epithelial deposits, drusen, thickened Bruch's membrane, and atrophy, hypopigmentation, and hyperpigmentation of the RPE.

Oxidative stress has long been linked to the pathogenesis of AMD. Imamura et al reported a Cu, Zn-superoxide dismutase (SOD1)-deficient mice that had features typical of AMD in human. Senescent Sod1 (-/-) mice had drusen, thickened Bruch's membrane, and choroidal neovascularization (Imamura, Noda, Hashizume, Shinoda, Yamaguchi, Uchiyama, Shimizu, Mizushima, Shirasawa, and Tsubota 2006). The number of drusen increased with age and also after exposure of young Sod1 (-/-) mice to excess light. The retinal pigment epithelial cells of Sod1 (-/-) mice showed oxidative damage, and their beta-catenin-mediated cellular integrity was disrupted. These findings suggested that oxidative stress may affect the junctional proteins necessary for the barrier integrity of the RPE. These observations strongly suggested that oxidative stress may play a major role in AMD.

The complement components, C3a and C5a, are present in drusen, and were observed in Bruch's membrane of a laser-induced CNV mice model. Neutralization of C3a or C5a by antibody or by blockade of their receptors by a complement inhibitor significantly reduced the CNV (Nozaki, Raisler, Sakurai, Sarma, Barnum, Lambris, Chen, Zhang, Ambati, Baffi, and Ambati 2006). These observations revealed a role for immunological mechanisms for the angiogenesis and provided evidence for future therapeutic strategies for AMD. Although the pathology of AMD is pronounced in the macula area, it is not confined to this region. Characteristics of human AMD such as thickening of Bruch's membrane, accumulation of drusen, and CNV have been observed in mouse models. Nevertheless, the primate model will still be the choice for AMD studies, especially at the stage when new therapeutic methods are tested and evaluated for the first time. However, it would be wise and more productive to study both primate and mouse models in AMD research. This will be necessary to learn the mechanisms underlying the disease and to identify clinical and molecular markers for the early stages of AMD. The findings from these studies will provide critical information needed to develop therapies for AMD.

7 Acknowledgements

This work was supported by the research grant from the Ministry of Health, Labour and Welfare of Japan.

References

Ambati, J., Anand, A., Fernandez, S., Sakurai, E., Lynn, B. C., Kuziel, W. A., Rollins, B. J., Ambati, B. K. (2003) An animal model of age-related macular degeneration in senescent Ccl-2- or Ccr-2-deficient mice. Nat. Med. 9, 1390-1397.

Chader, G. J. (2002) Animal models in research on retinal degenerations: Past progress and future hope. Vision Res 42, 393-399.

Dewan A., Liu, M., Hartman, S., Zhang, S. S., Liu, D. T., Zhao, C., Tam, P. O., Chan, W. M., Lam, D. S., Snyder, M., Barnstable, C., Pang, C. P., Hoh, J. (2006) HTRA1 promoter polymorphism in wet age-related macular degeneration. Science 314, 989-992.

Edwards, A. O., Ritter, R. 3rd., Abel, K. J., Manning, A., Panhuysen, C., Farrer, L. A. (2005) Complement factor H polymorphism and age-related macular degeneration. Science 308, 421-424.

El-Mofty A., Gouras, P., Eisner, G., Balazs, E. A. (1978) Macular degeneration in rhesus monkey (Macaca mulatta). Exp. Eye Res. 27, 499-502.

Gold, B., Merriam, J. E., Zernant, J., Hancox, L. S., Taiber, A. J., Gehrs, K., Cramer, K., Neel, J., Bergeron, J., Barile, G. R., Smith, R. T. (2006) AMD Genetics Clinical Study Group; G. S. Hageman, M. Dean, R. Allikmets. Variation in factor B (BF) and complement component 2 (C2) genes is associated with age-related macular degeneration. Nat. Genet. 38, 458-462.

Gotoh, N., Yamada, R., Hiratani, H., Renault, V., Kuroiwa, S., Monet, M., Toyoda, S., Chida, S., Mandai, M., Otani, A., Yoshimura, N., Matsuda, F. (2006) No association between complement factor H gene polymorphism and exudative age-related macular degeneration in Japanese. Hum. Genet. 120, 139-143.

Hageman, G. S., Anderson, D. H., Johnson, L. V., Hancox, L. S., Taiber, A. J., Hardisty, L. I., Hageman, J. L., Stockman, H. A., Borchardt, J. D., Gehrs, K. M., Smith, R. J., Silvestri, G., Russell, S. R., Klaver, C. C., Barbazetto, I., Chang, S., Yannuzzi, L. A., Barile, G. R., Merriam, J. C., Smith, R. T., Olsh, A. K., Bergeron, J., Zernant, J., Merriam, J. E., Gold, B., Dean, M., Allikmets, R. (2005) A common haplotype in the complement regulatory gene factor H (HF1/CFH) predisposes individuals to age-related macular degeneration. Proc. Natl. Acad. Sci. U S A 102, 7227-7232.

Haines, J. L., Hauser, M. A., Schmidt, S., Scott, W. K., Olson, L. M., Gallins, P., Spencer, K. L., Kwan, S. Y., Noureddine, M., Gilbert, J. R., Schnetz-Boutaud, N., Agarwal, A., Postel, E. A., Pericak-Vance, M. A. (2005) Complement factor H variant increases the risk of age-related macular degeneration. Science 308, 419-421.

Hammond, C. J., Webster, A. R., Snieder, H., Bird, A. C., Gilbert, C. E., Spector, T. D. (2002) Genetic influence on early age-related maculopathy: A twin study. Ophthalmology 109, 730-736.

Heiba, I. M., Elston, R. C., Klein, B. E., Klein, R. (1994) Sibling correlations and segregation analysis of age-related maculopathy: The Beaver Dam Eye Study. Genet. Epidemiol. 11, 51-67.

Imamura, Y., Noda, S., Hashizume, K., Shinoda, K., Yamaguchi, M., Uchiyama, S., Shimizu, T., Mizushima, Y., Shirasawa, T., Tsubota, K. (2006) Drusen, choroidal neovascularization, and retinal pigment epithelium dysfunction in SOD1-deficient mice: a model of age-related macular degeneration. Proc Natl Acad Sci U S A 103, 11282-11287.

Iyengar, S. K., Song, D., Klein, B. E., Klein, R., Schick, J. H., Humphrey, J., Millard, C., Liptak, R., Russo, K., Jun, G., Lee, K. E., Fijal, B., Elston, R. C. (2004) Dissection of genomewide-scan data in extended families reveals a major locus and oligogenic susceptibility for age-related macular degeneration. Am. J. Hum. Genet. 74, 20-39.

Klein, R. J., Zeiss, C., Chew, E. Y., Tsai, J. Y., Sackler, R. S., Haynes, C., Henning, A. K., SanGiovanni, J. P., Mane, S. M., Mayne, S. T., Bracken, M. B., Ferris, F. L., Ott, J., Barnstable, C., Hoh, J. (2005) Complement factor H polymorphism in age-related macular degeneration. Science 308, 385-389.

Schick, J. H., Iyengar, S. K., Klein, B. E., Klein, R., Reading, K., Liptak, R., Millard, C., Lee, K. E., Tomany, S. C., Moore, E. L., Fijal, B. A., Elston, R. C. (2003) A whole-genome screen of a quantitative trait of age-related maculopathy in sibships from the Beaver Dam Eye Study. Am. J. Hum. Genet. 72, 1412-1424.

Majewski, J., Schultz, D. W., Weleber, R. G., Schain, M. B., Edwards, A. O., Matise, T. C., Acott, T. S., Ott, J., Klein, M. L. (2003) Age-related macular degeneration--a genome scan in extended families. Am. J. Hum. Genet. 73, 540-550.

Malek, G., Johnson, L. V., Mace, B. E., Saloupis, P., Schmechel, D. E., Rickman, D. W., Toth, C. A., Sullivan, P. M., Bowes Rickman, C. (2005) Apolipoprotein E allele-dependent pathogenesis: a model for age-related retinal degeneration. Proc. Natl. Acad. Sci. U S A. 102, 11900-11905.

Mullins, R. F., Russell, S. R., Anderson, D. H., Hageman, G. S. (2000) Drusen associated with aging and age-related macular degeneration contain proteins common to extracellular deposits associated with atherosclerosis, elastosis, amyloidosis, and dense deposit disease. FASEB J 14, 835-846.

Nicolas, M. G., Fujiki, K., Murayama, K., Suzuki, M. T., Mineki, R., Hayakawa, M., Yoshikawa, Y., Cho, F., Kanai, A. (1996) Studies on the mechanism of early onset macular degeneration in cynomolgus (Macaca fascicularis) monkeys. I. Abnormal concentrations of two proteins in the retina. Exp. Eye Res. 62, 211-219.

Nicolas, M. G., Fujiki, K., Murayama, K., Suzuki, M. T., Shindo, N., Hotta, Y., Iwata, F., Fujimura, T., Yoshikawa, Y., Cho, F., Kanai, (1996) A. Studies on the mechanism of early onset macular degeneration in cynomolgus monkeys. II. Suppression of metallothionein synthesis in the retina in oxidative stress. Exp. Eye Res. 62, 399-408.

Nozaki, M., Raisler, B. J., Sakurai, E., Sarma, J. V., Barnum, S. R., Lambris, J. D., Chen, Y., Zhang, K., Ambati, B. K., Baffi, J. Z., Ambati J. (2006) Drusen complement components C3a and C5a promote choroidal neovascularization. Proc. Natl. Acad. Sci. U S A 103, 2328-2333.

Okamoto, H., Umeda, S., Obazawa, M., Minami, M., Noda, T., Mizota, A., Honda, M., Tanaka, M., Koyama, R., Takagi, I., Sakamoto, Y., Saito, Y., Miyake, Y., Iwata, T. (2006) Complement factor H polymorphisms in Japanese population with age-related macular degeneration. Mol. Vis. 12, 156-158.

Russell, S. R., Mullins, R. F., Schneider, B. L., Hageman, G. S. (2000) Location, substructure, and composition of basal laminar drusen compared with drusen associated with aging and age-related macular degeneration. Am J Ophthalmol 129, 205-214.

Seddon, J. M., Ajani, U. A., Mitchell, B. D. (1997) Familial aggregation of age-related maculopathy. Am. J. Ophthalmology 123, 199-206.

Stafford, T. J., Anness, S. H., Fine, B. S. (1984) Spontaneous degenerative maculopathy in the monkey. Ophthalmology 91, 513-521.

Yang, Z., Camp, N. J., Sun, H., Tong, Z., Gibbs, D., Cameron, D. J., Chen, H., Zhao, Y., Pearson, E., Li, X., Chien, J., Dewan, A., Harmon, J., Bernstein, P. S., Shridhar, V., Zabriskie, N. A., Hoh, J., Howes, K., Zhang, K.. (2006) A variant of the HTRA1 gene increases susceptibility to age-related macular degeneration. Science. 314, 992-993.

Umeda, S., Ayyagari, R., Allikmets, R., Suzuki, M. T., Karoukis, A. J., Ambasudhan, R., Zernant, J., Okamoto, H., Ono, F., Terao, K., Mizota, A., Yoshikawa, Y., Tanaka, Y., Iwata, T. (2005) Early-onset macular degeneration with drusen in a cynomolgus monkey (Macaca fascicularis) pedigree: exclusion of 13 candidate genes and loci. Invest. Ophthalmol. Vis. Sci. 46, 683-691.

Umeda, S., Suzuki, M. T., Okamoto, H., Ono, F., Mizota, A., Terao, K., Yoshikawa, Y., Tanaka, Y., Iwata, T. (2005) Molecular composition of drusen and possible involvement of anti-retinal autoimmunity in two different forms of macular degeneration in cynomolgus monkey (Macaca fascicularis). FASEB J. 19, 1683-1685.

Proteomic and Transcriptomic Analyses of Retinal Pigment Epithelial Cells Exposed to REF-1/TFPI-2

Masahiko Shibuya,[1,2] *Haru Okamoto,*[1] *Takehiro Nozawa,*[3] *Jun Utsumi,*[4] *Venkat N. Reddy,*[5] *Hirotoshi Echizen,*[2] *Yasuhiko Tanaka,*[6] *and Takeshi Iwata*[1]

PURPOSE. The authors previously reported a growth-promoting factor, REF-1/TFPI-2, that is specific to retinal pigment epithelial (RPE) cells. The purpose of this study was to determine the genes and proteins of human RPE cells that are altered by exposure to TFPI-2.

METHODS. Human primary RPE cells were cultured with or without TFPI-2. Cell extracts and isolated RNA were subjected to proteomic and transcriptomic analyses, respectively. Proteins were separated by two-dimensional gel electrophoresis followed by gel staining and ion spray tandem mass spectrometry analyses. Transcriptomic analysis was performed using a DNA microarray to detect 27,868 gene expressions.

RESULTS. Proteomic analysis revealed c-Myc binding proteins and ribosomal proteins L11 preferentially induced by TFPI-2 in human RPE cells. Transcriptomic analysis detected 10,773 of 33,096 probes in the TFPI-2 treated samples, whereas only 2186 probes were detected in the nontreated samples. Among the genes up-regulated by TFPI-2 at the protein level were c-*myc*, Mdm2, transcription factor E2F3, retinoblastoma binding protein, and the *p21* gene, which is associated with the c-*myc* binding protein and ribosomal protein L11.

CONCLUSIONS. The mechanisms by which TFPI-2 promotes the proliferation of RPE cells may be associated with augmented c-*myc* synthesis and the activation of E2F in the retinoblastoma protein (Rb)/E2F pathway at the G1 phase of the RPE cells. Activation of ribosomal protein L11 and the Mdm2 complex of the p53 pathway may be counterbalanced by the hyperproliferative conditions. (*Invest Ophthalmol Vis Sci.* 2007;48: 516–521) DOI:10.1167/iovs.06-0434

Retinal pigment epithelial (RPE) cells play important roles in maintaining the homeostasis of the retina. RPE cells, located between the sensory retina and the choroidal blood supply, form a diffusion barrier controlling access to the subretinal space, with the RPE membrane regulating the transport of proteins and controlling the hydration and ionic composition of the subretinal space. The sensitivity and viability of the photoreceptors thus depend on RPE-catalyzed transport activity. Proteins in the RPE cells that function in ionic, sugar, peptide, and water transport have been identified.[1] Damage to RPE cells generally leads to degeneration of the neural retina, as occurs in retinitis pigmentosa and age-related macular degeneration. Transplantation of the healthy retinal pigment cells or embryonic stem cells differentiating into RPE cells would be an ideal therapeutic approach to treat such diseases, and such attempts have been made.[2]

An alternative approach to treat these retinal diseases would be the use of a growth factor that promotes proliferation of the remaining RPE cells in a damaged retina or one that stimulates the regeneration of damaged RPE cells. To find such factor(s), the proteins expressed in human fibroblast cells were fractionated and assayed, leading to the isolation of RPE cell factor-1 (REF-1), which selectively promoted the proliferation of primary human RPE cells.[3]

Subsequently, the cDNA of REF-1 was cloned using information from the N-terminal amino acid sequences, which was identical with the tissue factor pathway inhibitor-2 (TFPI-2).[3] Earlier studies have shown that TFPI-2 is a Kunitz-type serine protease inhibitor[4–6] involved in the regulation of extrinsic blood coagulation[4,7] and in the proliferation, invasion, and metastasis of various types of malignant cells.[4,8–13] Extensive studies on the physiological roles of TEPI-2 have revealed that the ERK/MAPK pathway[13] may be associated with the up-regulation of the *TFPI-2* gene and that DNA methylation[9,10] in certain tumor cell lines may be related to the downregulation of the *TEPI-2* gene. When TFPI-2 is added to the culture medium of vascular smooth muscle cells, it promotes cell proliferation.[14]

Our initial finding that TFPI-2 enhanced RPE proliferation prompted us to question how this was achieved. We applied proteomic and transcriptomic analyses to screen the changes in the expression of the RNAs and proteins in RPE cells and will show that the proliferation promoting activity of TFPI-2 on RPE cells is associated with the regulation of an oncogene product, c-*myc*, and representative cancer repressor proteins retinoblastoma protein (Rb)/E2F and p53.

MATERIALS AND METHODS

TFPI-2 Treatment of Human RPE Cell Culture

Human primary RPE cells (passage 5) were seeded at a density of 2.5×10^4 cells/0.5 mL per well in 24-well plastic plates (BD Biosciences, Franklin Lakes, NJ) with Dulbecco modified MEM (DMEM; Invitrogen Japan, Tokyo, Japan) containing 15% fetal calf serum (FCS, Invitrogen). TFPI-2 was added to 20 wells with the RPE cells at 10 ng/mL concentrations and was incubated at 37°C for 24 hours for the proteomic samples, and for 6 hours, 12 hours, and 24 hours for the transcriptomic samples. An equal amount of saline was added to 20 wells containing RPE cells for controls. TFPI-2 was donated by Toray Industries, Inc., Tokyo, Japan.

From the [1]Laboratory of Cellular and Molecular Biology, National Institute of Sensory Organs, National Hospital Organization Tokyo Medical Center, Tokyo, Japan; [2]Department of Pharmacotherapy, Meiji Pharmaceutical University, Tokyo, Japan; [3]Analytical Instrument Division, AMR Inc., Tokyo, Japan; [4]R&D Division, Toray Industries, Inc., Tokyo, Japan; [5]Department of Ophthalmology, Kellogg Eye Center, University of Michigan, Ann Arbor, Michigan; and [6]International University of Health and Welfare, Mita Hospital, Tokyo, Japan.

Supported in part by a grant-in-aid from the policy-based Medical Services Foundation.

Submitted for publication April 18, 2006; revised July 17, 2006; accepted December 4, 2006.

Disclosure: **M. Shibuya**, None; **H. Okamoto**, None; **T. Nozawa**, AMR Inc. (F); **J. Utsumi**, Toray Industries, Inc. (F); **V.N. Reddy**, None; **H. Echizen**, None; **Y. Tanaka**, None; **T. Iwata**, None

The publication costs of this article were defrayed in part by page charge payment. This article must therefore be marked "*advertisement*" in accordance with 18 U.S.C. §1734 solely to indicate this fact.

Corresponding author: Takeshi Iwata, Laboratory of Cellular and Molecular Biology, National Institute of Sensory Organs, National Hospital Organization Tokyo Medical Center, 2-5-1 Higashigaoka, Meguro-ku, Tokyo 152-8902, Japan; iwatatakeshi@kankakuki.go.jp.

Investigative Ophthalmology & Visual Science, February 2007, Vol. 48, No. 2

Protein Sample Preparation

To isolate whole cellular protein extracts from cultured RPE cells, the cells were rinsed 3 times with 1× PBS (pH 7.4) and were lysed in a denaturing lysis buffer containing 7 M urea, 2 M thiourea, 4% CHAPS, 40 mM Tris, 0.2% purifier (Bio-Lyte, pH range 3–10; Bio-Rad, Hercules, CA), and 50 mM dithiothreitol (DTT). The collected lysate was then centrifuged at 14,000*g* for 15 minutes at 4°C. Proteins in the supernatant were repeatedly concentrated and precipitated and finally desalinated (Readyprep 2-D Cleanup kit; Bio-Rad). The protein concentration in the RPE samples was determined by a modified Lowry method adapted for use with the lysis buffer.

Two-Dimensional Electrophoresis

Protein samples were separated by a two-dimensional electrophoresis method. A 300-μg protein sample was loaded on immobilized pH gradient (IPG) strips (pH 3–10, 7 cm; pH 4–7, 17 cm; Bio-Rad) by in-gel rehydration at 20°C overnight. For the 7-cm strip, isoelectric focusing (IEF) was used for the first dimension at an initial voltage of 250 V for 15 minutes, increased to 4000 V for 2 hours, and held until 20,000 V/h was reached. For the 17-cm strip, the initial voltage was set at 250 V, as for the 7-cm strip. Then the voltage was increased to 10,000 V for 3 hours and was held until 60,000 V/h was reached. Immediately after IEF, the IPG strips were equilibrated for 20 minutes in buffer containing 6 M urea, 2% SDS, 0.375 M Tris (pH 8.8), and 20% glycerol under a reduced condition with 2% DTT (Bio-Rad), followed by another incubation for 10 minutes in the same buffer under alkylating conditions with 2.5% iodoacetamide (Bio-Rad).[15]

Equilibrated IPG strips were then electophoresed by SDS-PAGE for the second dimension. Images of the chemiluminescent signals were captured and merged with those of protein spots made visible by protein gel stain (Sypro Ruby; Bio-Rad), and the spots corresponding to the immunoreactivity were cut out. To test reproducibility, the experiment was performed twice.

Protein Identification by Mass Spectrometry

Excised gel pieces were rinsed with water and then with acetonitrile and were completely dried for the reduction-alkylation step. They were incubated with 10 mM DTT in 100 mM ammonium bicarbonate for 45 minutes at 56°C, then with 55 mM iodoacetamide in 100 mM ammonium bicarbonate for 30 minutes at room temperature in the dark. The supernatant was removed, and the washing procedure was repeated three times. Finally, the gel pieces were again completely dried before trypsin digestion and were rehydrated in a solution of trypsin (12.5 ng/μL; Promega, Madison, WI) in 50 mM ammonium bicarbonate. The digestion was continued for 16 hours at 37°C, and the extraction step was performed once with 25 mM ammonium bicarbonate, then twice with 5% formic acid, and finally with water. After resuspension in 40 μL solution of aqueous 0.1% trifluoroacetic acid/2% acetonitrile, the samples were analyzed by liquid chromatography coupled to tandem mass spectrometry (LC-MS/MS). For analysis by LC-MS/MS, the tryptic digests were injected by an automatic sampler (HTS-PAL, CTC Analytics, Zwingen, Switzerland) onto a 0.2 × 50-mm capillary reversed-phase column (Magic C18, 3 μm; Michrom BioResources, Inc., Auburn, CA) using an HPLC (Paradigm MS4; Michrom BioResources). Peptides were eluted with a gradient (95% solvent A consisting of 98% H_2O/2% acetonitrile/0.1% formic acid)/5% solvent B (10% H_2O/90% acetonitrile/0.1% formic acid; 0 minute)/35% solvent A/65% solvent B (20 minutes)/5% solvent A/95% solvent B (21 minutes)/5% solvent A/95% solvent B (23 minutes)/95% solvent A/5% solvent B (30 minutes) for 30 minutes at a flow rate of 1.5 μL/min. Peptides were eluted directly into an ion trap mass spectrometer (ESI; Finnigan LTQ; Thermo Electron Corporation, Waltham, MA) capable of data-dependent acquisition. Each full MS scan was followed by an MS/MS scan of the most intense peak in the full MS spectrum with the dynamic exclusion enabled to allow detection of less-abundant peptide ions. Mass spectrometric scan events and HPLC solvent gradients were controlled with the use of a computer program (Paradigm Home; Michrom BioResources).

Total RNA Isolation from RPE Cells

Total RNA was isolated from the cultured RPE cells after 6 hours, 12 hours, and 24 hours with TFPI-2 using a total RNA isolation kit (RNA-Bee-RNA Isolation Reagent; Tel-Test, Friendswood, TX). Total RNA samples were treated with RNase-free DNase (Roche Diagnostics Japan) to minimize genomic DNA contamination.

DNA Microarray Analysis

DNA microarray analysis was performed (AB1700 Chemiluminescent Microarray Analyzer; Applied Biosystems, Foster City, CA). The survey array used (Human Genome Survey Array; Applied Biosystems) contained 33,096 60-mer oligonucleotide probes representing a set of 27,868 individual human genes and more than 1000 control probes. Sequences used for the microarray probe were obtained from curated transcripts (Celera Genomics Human Genome Database), RefSeq transcripts that had been structurally curated from the LocusLink public database, high-quality cDNA sequences from the Mammalian Gene Collection (MGC; http://mgc.nci.nih.gov), and transcripts that were experimentally validated (Applied Biosystems). The 60-mer oligo probes were synthesized using standard phosphoramidite chemistry and solid-phase synthesis and underwent quality control by mass spectrometry. The probes were deposited and covalently bound to a derivatized nylon substrate (2.5 × 3 inches) that was backed by a glass slide by contact spotting with a feature diameter of 180 μm and more than 45 μm between each feature. A 24-mer oligo internal control probe (ICP) was cospotted at every feature with 60-mer gene expression probe on the microarray. Digoxigenin-UTP labeled cRNA was generated and linearly amplified from 1 μg total RNA (Chemiluminescent RT-IVT Labeling Kit, version 2.0; Applied Biosystems) according to the manufacturer's protocol. Array hybridization (two arrays per sample), chemiluminescence detection, image acquisition, and analysis were performed (Chemiluminescence Detection Kit and AB1700 Chemiluminescent Microarray Analyzer; Applied Biosystems) according to the manufacturer's protocol.

Briefly, each microarray was first prehybridized at 55°C for 1 hour in hybridization buffer with blocking reagent. Sixteen micrograms labeled cRNA targets were first fragmented into 100 to 400 bases by incubation with fragmentation buffer at 60°C for 30 minutes, mixed with internal control target (ICT; 24-mer oligo labeled with LIZR fluorescent dye), and hybridized to each prehybrid microarray in 1.5 mL vol at 55°C for 16 hours. After hybridization, the arrays were washed with hybridization wash buffer and chemiluminescence rinse buffer. Enhanced chemiluminescent signals were generated by first incubating the arrays with anti-digoxigenin alkaline phosphatase and enhanced with chemiluminescence enhancing solution and chemiluminescence substrate.

Images were collected from each microarray using the 1700 analyzer equipped with a high-resolution, large-format CCD camera, including 2 "short" chemiluminescent images (5-second exposure length each) and 2 "long" chemiluminescent images (25-second exposure length each) for gene expression analysis, two fluorescent images for feature finding and spot normalization, and two quality control images for spectrum cross-talk correction. Images were quantified, corrected for background and spot, and spatially normalized.

Data Analysis

MS data were identified with the use of a protein search program (BioWorks 3.2; Thermo Electron Corporation, Waltham, MA). For protein database searches, the same program was used to create centroid peak lists from the raw spectra. These peak lists were then submitted for database searching (BioWorks). The identity of the samples was searched from databases (nrNCBI [www.ncbi.nlm.nih.gov]) that extracted proteins and were restructured; search terms included human and *Homo sapiens*. Differentially expressed proteins were further analyzed for related genes and proteins using natural language processing software (Pubgene database; PubGene Inc., Boston, MA) and data mining software of gene expression (OmniViz; OmniViz, Inc., Maynard, MA).

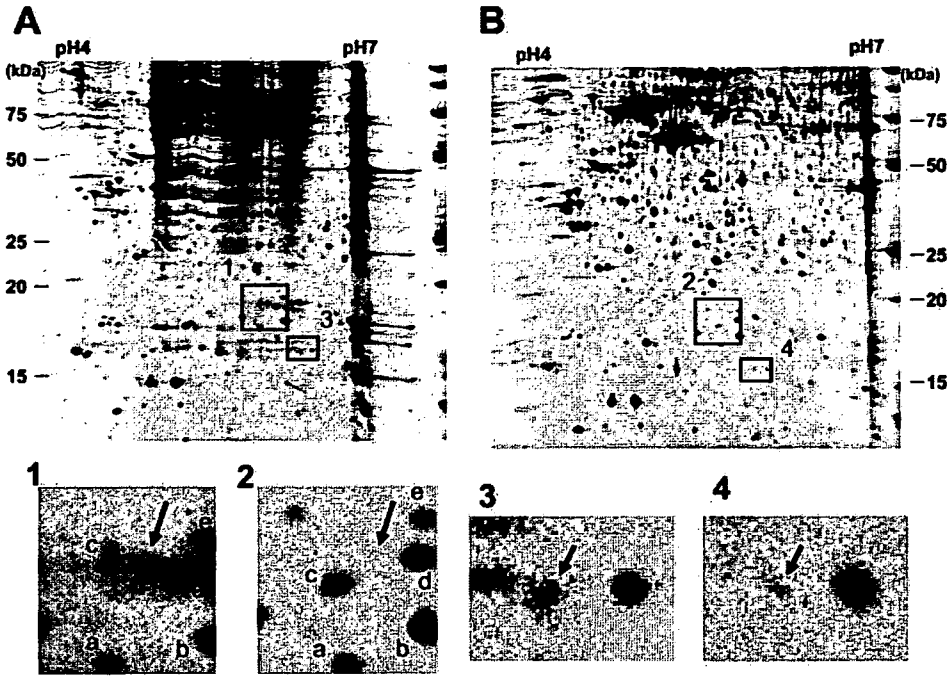

FIGURE 1. Two-dimensional gel electrophoresis of human RPE cells culture with (A) and without (B) TFPI-2. Spots corresponding to proteins whose expression is dependent on the presence of TFPI-2 in the culture medium are indicated by the *arrows* (*insets*). Proteins were detected by SYPRO Ruby staining. Spots corresponding to the differentially expressed proteins indicated by *arrows* (1 vs. 2 and 3 vs. 4) were subsequently subject to the LC-MS/MS analysis so that proteins could be identified.

RESULTS

Proteome Analysis of RPE Cells Treated with TFPI-2

To determine the mechanisms responsible for the proliferation-promoting activity of TFPI-2 on RPE cells, protein synthesis and RNA expression were determined before and after TFPI-2 exposure. Differentially expressed proteins in the primary human RPE cells in response to TFPI-2 were identified by two-dimensional electrophoresis (Fig. 1). Samples were initially separated using IPG at a pH range of 3 to 10 to observe the full distribution of protein spots. The pH range was then narrowed to 4 to 7 to obtain higher resolution for spot picking. Consequently, approximately 480 spots were identified in the whole gel. We then focused on molecular weight less than 25 kDa, which is easy to check for changes. Ten spots considered differentially expressed in the two-dimensional gel were collected and subjected to LC-MS/MS analysis. Among the identified proteins, ribosomal protein L11 (RPL11; Fig. 1-1) and c-Myc binding protein (MYCBP; Fig. 1-3), known for regulating cell proliferation, were identified.[16] These two proteins, identified by LC-MS/MS analysis and data analysis software (Bioworks 3.2), were consistent with those estimated from the results of two-dimensional electrophoresis (Table 1).

Transcriptomic Analysis of RPE Cells Treated with TFPI-2

The expression of 8134 genes in RPE cells was analyzed using DNA microarray with and without TFPI-2 exposure for 6 hours, 12 hours, and 24 hours. Signal normalization was performed for six independent DNA microarray chips according to the manufacturer's protocol. Genes differentially expressed by more than threefold were considered significant and were selected for further analysis. Among the 33,096 possible probes, 10,773 probes were detected in the RPE cells incubated with TFPI-2, whereas only 2186 probes were detected without TFPI-2. Based on expression levels at the three time points (6 hours, 12 hours, and 24 hours), the time-dependent expression pattern of each gene was calculated and clustered with other genes with similar expression patterns using data mining software (OmniViz). Data analysis resulted in 38 clusters of genes that either increased or decreased their expression levels by more than twofold after TFPI-2 (Fig. 2). Nineteen genes were upregulated in 5 clusters, 108 genes in 16 clusters, and 717 genes in 22 clusters at 6 hours, 12 hours, and 24 hours, respectively. For downregulated genes, 30 genes in 16 clusters, 119 genes in 19 clusters, and 3 genes in 19 clusters were observed after 6 hours, 12 hours, and 24 hours, respectively. Transcriptomic analysis revealed significantly more genes differentially expressed at the transcriptional level than at the proteome level.

DISCUSSION

Proteins and genes whose expression was upregulated or downregulated after exposure to TFPI-2 were analyzed in human RPE cells to study the proteomic and transcriptomic changes. Protein and gene expression profiles for human RPE cells have been reported by West et al.,[17] who identified 278 proteins, and Cai et al.,[18] who reported 5580 ± 84 genes expressed in adult human RPE and ARPE19 cell lines using a DNA chip with 12,600 probes (Human U95Av2; Affymetrix, Santa Clara, CA). Our study showed changes in the expression of 8134 of 27,868 genes. DNA microarray analyses were simul-

TABLE 1. Two-Dimensional Gel Spots Identified by Mass Spectrometry

Protein	Number of AA	Peptide Residues	Identified Peptide from Database	MW	Score	Accession Number
c-Myc binding protein	167	108–117	TAEDAKDFFK	18642.6	10.13	1731809
Ribosomal protein L11	177	88–94	VREYELR	20125.1	20.21	14719845

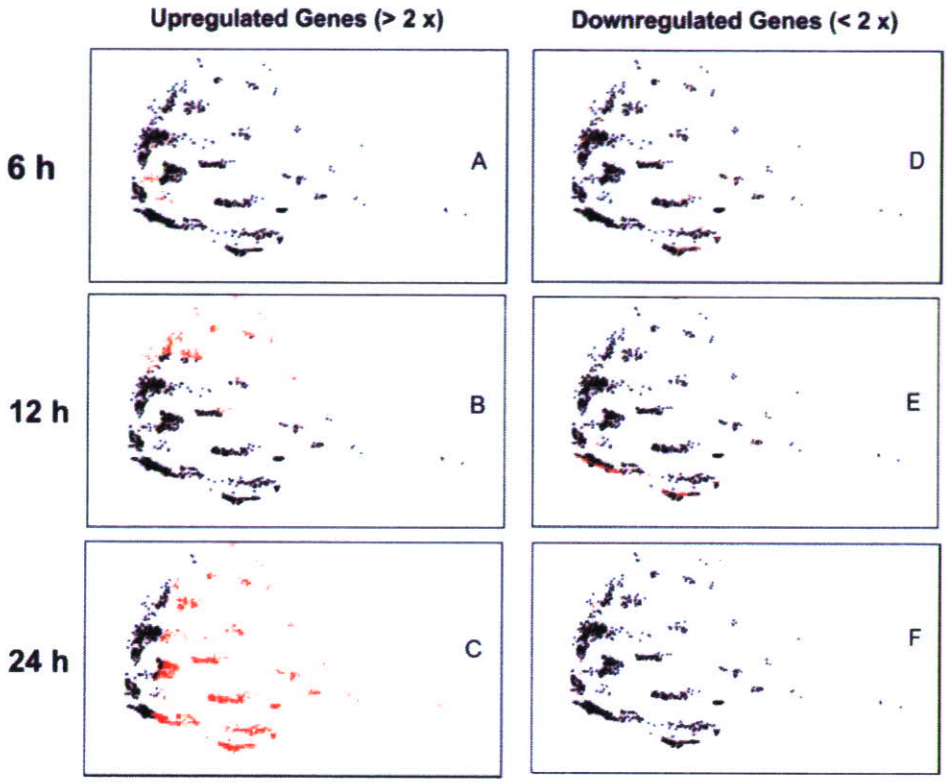

FIGURE 2. Differentially expressed genes detected by DNA array are plotted as clusters. Differentially expressed genes whose expression level was increased by more than twofold (**A**–**C**) or was reduced by more than 0.5-fold (**D**–**F**) in RPE cells treated with TFPI-2 at incubation times of 6 hours, 12 hours, and 24 hours compared with the control cells are shown. Expression profile analysis revealed different gene expression patterns at each incubation time.

taneously performed at three time points (6 hours, 12 hours, and 24 hours) to monitor the course of expression of the possible 27,868 genes in human RPE cells exposed and not exposed to TFPI-2. This study was conducted at the translational and the transcriptional levels to complement the disadvantages of each method.

Raw gene expression data were further analyzed with data mining software (OmniViz) to obtain an overall picture of the transcriptional changes induced by TFPI-2 in human primary RPE cells. Genes whose expressions were changed by more than twofold were clustered into 38 groups showing a change of expression at each time point (Fig. 2). The number of genes upregulated at each time point was considerably higher than the number that was downregulated. A small number of genes was triggered by TFPI-2 treatment at 6 hours, before the major changes occurred at 24 hours. Among the initially upregulated genes were reticulon 4 interacting protein 1, phospholipase C, delta 1, granzyme M (lymphocyte met-ase 1; *GZMM*), and mitochondrial ribosomal protein L41 (*MRPL41*).

Proteomics analysis simultaneously performed at 24 hours identified two differentially expressed proteins, the c-*myc* binding protein (MYCBP) and the ribosomal protein L11 (RPL11). MYCBP and RPL11 (Fig. 3) are well known to regulate cell cycling through the Rb/E2F pathway and the p53 pathway, respectively. MYCBP stimulates c-*myc* transcription through the retinoblastoma protein (Rb)/E2F pathway (see Fig. 5). Sears et al.[19] reported that activation of Myc increased the signal transduction of the cyclin D/cdk4 and cyclin E/cdk2 pathways. Activation of these pathways inactivates Rb after phosphorylation and E2F dissociation, which then promotes RPE cells to go into the S-phase of the cell cycle. The twofold transcriptional increase of *Rb* and *E2F3* in TFPI-2 exposed cells compared with control at 24 hours supports this hypothesis (Figs. 4C, 4F).

Concomitantly, the expressions of Rb and Mdm2 were upregulated twofold in growth-stimulated cells compared with control cells. Because Rb is associated with the negative regulation of the G_1-phase of the cell cycle, the enhanced expres-

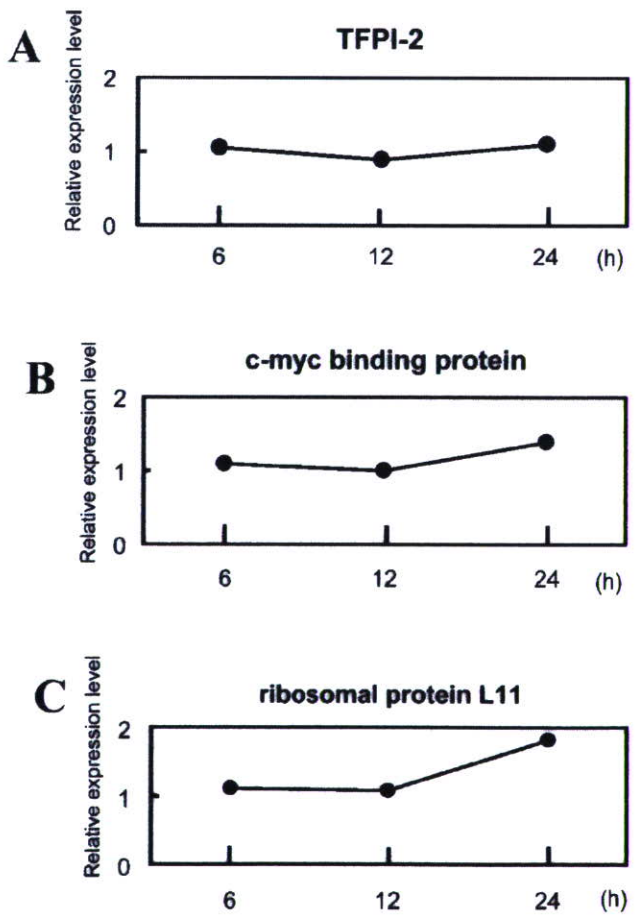

FIGURE 3. Time course of gene expression for TFPI-2 (**A**), c-*myc* binding protein (**B**), and ribosomal protein L11 (**C**) in the cultured human RPE cells after exposure to TFPI-2.

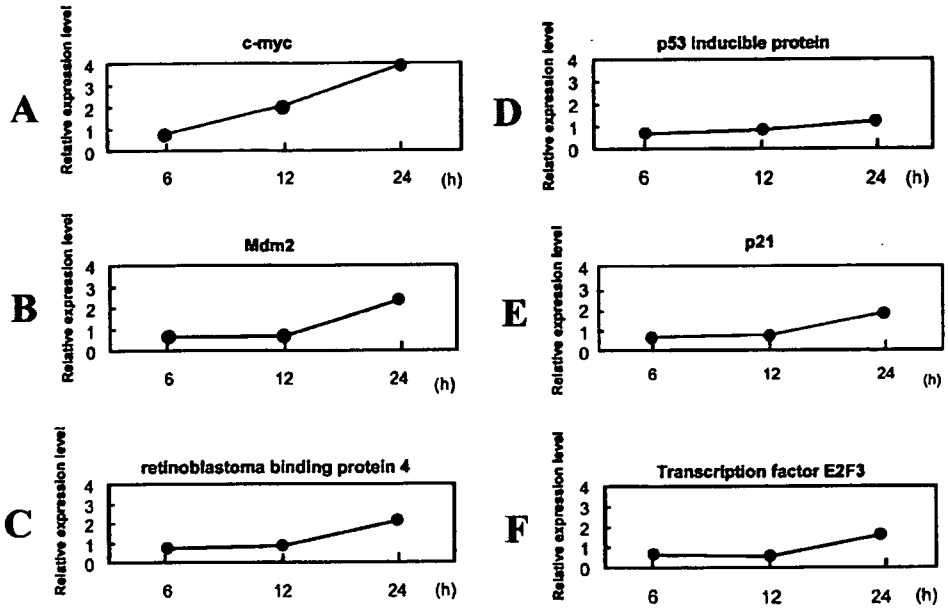

FIGURE 4. Time courses of protein expression patterns for c-*myc* (A), Mdm2 (B), retinoblastoma binding protein 4 (C), p-53 inducible protein (D), p21 (E), and transcription factor E2F3 in the cultured human RPE cells after exposure to TFPI-2.

sion of *Mdm2* might have been involved in the augmented degradation of Rb through the ubiquitin/proteasome-dependent pathway. Recently, Uchida et al.[20] suggested that Mdm2 regulates the function of RB through the ubiquitin-dependent degradation of RB.

The *Rb* gene was the first identified tumor-suppressor gene,[21] and it was recognized as a central component of a signaling pathway that controlled cell proliferation. Specifically, the D-type G_1 cyclins, together with their associated cyclin-dependent kinases (CKDs) Cdk4 and Cdk6, initiated the phosphorylation of Rb and Rb family members, inactivating their capacity to interact with the E2F transcription factors (Fig. 5).[19] This phosphorylation leads to an accumulation of E2F1, E2F2, and E2F3a, which activate the transcription of a large number of genes essential for DNA replication and further cell cycle progression.[22-26] Among the E2F targets are genes encoding a second class of G_1 cyclins, cyclin E, and the associated kinase Cdk2 (Fig. 5).[19] The activation of cyclin E/Cdk2 kinase activity by E2F leads to further phosphorylation and inactivation of Rb, further enhancing E2F activity and increasing the accumulation of cyclin E/Cdk2 (Fig. 5).[19] This feedback loop, which leads to a continual inactivation of *Rb* independent of the action of cyclin D/Cdk4—defined as a junction in cell proliferation response when passaged through the cell cycle—becomes growth factor independent.[25,26] The activity of the G_1 Cdks is negatively regulated by a family of cyclin-dependent kinase inhibitors (CKIs), including $p21^{WAF1}$, $p27^{Kip1}$, and the $p16^{INK4a}$ family.[27] The three upregulated E2Fs associate exclusively with Rb and appear to play a positive role in cell cycle progression.[19]

RPL11 binds the mouse double-minute 2 (Mdm2 is the mouse homologue of Hdm2 in humans) protein with other ribosomal proteins (L23 and L5) to form a complex to inhibit ubiquitin-dependent degradation of p53.[28-30] The RPL11 protein is expressed in ARPE-19 cells.[31] Inhibition of p53 degradation leads to p21 signaling, which participates in the G_1

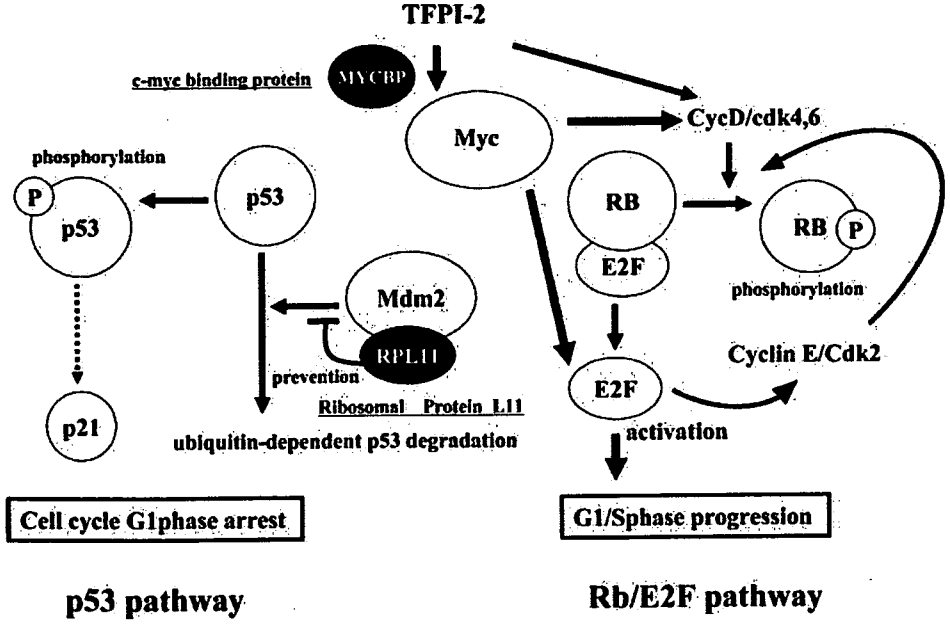

FIGURE 5. Hypothetical network of various genes and proteins associated with the growth-promoting effect of TFPI-2 on the human RPE cells. *Arrows*: stimulatory signals. *Straight* and *dotted lines*: inhibitory effects.

arrest of the cell cycle but also negatively regulates cell proliferation (Fig. 5).[30,32-34] In support of this hypothesis, *p21* transcription was increased by twofold after 24 hours by TFPI-2.

The *p53* gene mediates a major tumor-suppression pathway in mammalian cells and is frequently altered in human tumors.[30] Its function is kept at a low level during normal cell growth and is activated in response to various cellular stresses by acting as a sequence-specific transcription factor.[30] The p53 protein induces cell cycle arrest or apoptosis.[30]

Shinoda et al.[14] reported cell growth proliferation of vascular smooth muscle endothelial cells by a purified mitogenic substance from human umbilical vein endothelial cells, later identified as TFPI-2. These authors showed the rapid activation of mitogen-activated protein kinase (MAPK) by TFPI-2 and the induced activation of proto-oncogene *c-fos* mRNA in smooth muscle cells.[14] They concluded that *c-fos* activation was initiated by MAPK based on MAPK inhibitor PD098059 suppression.

In conclusion, the results of proteomic and transcriptomic analyses suggest that the proliferation of RPE cells induced by TFPI-2 is regulated through the Rb/E2F, p53, and Ras/Raf/MAPK pathways. We and others[3,35] have reported a transcript of TFPI-2 in the mRNA of RPE cells. It is now reasonable to expect that RPE cells are able to self-proliferate by generating TFPI-2. Additional studies are needed to determine whether TFPI-2 can act as such an autocrine factor and can be modified for future treatment of the dry-type age-related macular degeneration and of retinitis pigmentosa.

References

1. Hughes BA, Gallemore RP, Miller SS. Transport mechanisms in the retinal pigment epithelium. In: Marmor MF, Wolfensberger TJ, eds. *The Retinal Pigment Epithelium: Function and Disease*. New York: Oxford University Press; 1998:103-134.
2. Haruta M. Embryonic stem cells: potential source for ocular repair. *Semin Ophthalmol*. 2005;20:17-23.
3. Tanaka Y, Utsumi J, Matsui M, et al. Purification, molecular cloning, and expression of a novel growth-promoting factor for retinal pigment epithelial cells, REF-1/TFPI-2. *Invest Ophthalmol Vis Sci*. 2004;45:245-252.
4. Chand HS, Foster DC, Kisiel W. Structure, function and biology of tissue factor pathway inhibitor-2. *Thromb Haemost*. 2005;94:1122-1130.
5. Schmidt AE, Chand HS, Cascio D, et al. Crystal structure of Kunitz domain 1 (KD1) of tissue factor pathway inhibitor-2 in complex with trypsin: implications for KD1 specificity of inhibition. *J Biol Chem*. 2005;280:27832-27838.
6. Chand HS, Schmidt AE, Bajaj SP, et al. Structure-function analysis of the reactive site in the first Kunitz-type domain of human tissue factor pathway inhibitor-2. *J Biol Chem*. 2004;279:17500-17507.
7. Sprecher CA, Kisiel W, Mathewes S, et al. Molecular cloning, expression, and partial characterization of a second human tissue-factor-pathway inhibitor. *Proc Natl Acad Sci USA*. 1994;91:3353-3357.
8. Yanamandra N, Kondraganti S, Gondi CS, et al. Recombinant adeno-associated virus (rAAV) expressing TFPI-2 inhibits invasion, angiogenesis and tumor growth in a human glioblastoma cell line. *Int J Cancer*. 2005;115:998-1005.
9. Rollin J, Iochmann S, Blechet C, et al. Expression and methylation status of tissue factor pathway inhibitor-2 gene in non-small-cell lung cancer. *Br J Cancer*. 2005;92:775-783.
10. Konduri SD, Srivenugopal KS, Yanamandra N. Promoter methylation and silencing of the tissue factor pathway inhibitor-2 (TFPI-2), a gene encoding an inhibitor of matrix metalloproteinases in human glioma cells. *Oncogene*. 2003;22:4509-4516.
11. Santin AD, Zhan F, Bignotti E, et al. Gene expression profiles of primary HPV16- and HPV18-infected early stage cervical cancers and normal cervical epithelium: identification of novel candidate molecular markers for cervical cancer diagnosis and therapy. *Virology*. 2005;331:269-291.
12. Sato N, Parker AR, Fukushima N, et al. Epigenetic inactivation of TFPI-2 as a common mechanism associated with growth and invasion of pancreatic ductal adenocarcinoma. *Oncogene*. 2005;24:850-858.
13. Kast C, Wang M, Whiteway M. The ERK/MAPK pathway regulates the activity of the human tissue factor pathway inhibitor-2 promoter. *J Biol Chem*. 2003;278:6787-6794.
14. Shinoda E, Yui Y, Hattori R, et al. Tissue factor pathway inhibitor-2 is a novel mitogen for vascular smooth muscle cells. *J Biol Chem*. 1999;274:5379-5384.
15. Bahk SC, Lee SH, Jang JU, et al. Identification of crystallin family proteins in vitreous body in rat endotoxin-induced uveitis: involvement of crystallin truncation in uveitis pathogenesis. *Proteomics*. 2006;6:3436-3444.
16. Taira T, Maëda J, Onishi T, et al. AMY-1, a novel C-MYC binding protein that stimulates transcription activity of C-MYC. *Genes Cells*. 1998;3:549-565.
17. West KA, Yan L, Shadrach K, et al. Protein database, human retinal pigment epithelium. *Mol Cell Proteomics*. 2003;2:37-49.
18. Cai H, Del Priore LV. Gene expression profile of cultured adult compared to immortalized human RPE. *Mol Vis*. 2006;12:1-14.
19. Scars RC, Nevins JR. Signaling networks that link cell proliferation and cell fate. *J Biol Chem*. 2002;277:11617-11620.
20. Uchida C, Miwa S, Kitagawa K, et al. Enhanced Mdm2 activity inhibits pRB function via ubiquitin-dependent degradation. *EMBO J*. 2005;24:160-169.
21. Hanahan D, Weinberg RA. The hallmarks of cancer. *Cell*. 2000;100:57-70.
22. Dyson N. The regulation of E2F by pRB-family proteins. *Genes Dev*. 1998;12:2245-2262.
23. Nevins JR. Toward an understanding of the functional complexity of the E2F and retinoblastoma families. *Cell Growth Differ*. 1998;9:585-593.
24. Harbour JW, Dean DC. Rb function in cell-cycle regulation and apoptosis. *Nat Cell Biol*. 2000;2:E65-E67.
25. Dou QP, Levin AH, Zhao S, Pardee AB. Cyclin E and cyclin A as candidates for the restriction point protein. *Cancer Res*. 1993;53:1493-1497.
26. Pardee AB. A restriction point for control of normal animal cell proliferation. *Proc Natl Acad Sci USA*. 1974;71:1286-1290.
27. Sherr CJ, Roberts JM. CDK inhibitors: positive and negative regulators of G1-phase progression. *Genes Dev*. 1999;13:1501-1512.
28. Krystof V, McNae IW, Walkinshaw MD. Antiproliferative activity of olomoucine II, a novel 2,6,9-trisubstituted purine cyclin-dependent kinase inhibitor. *Cell Mol Life Sci*. 2005;62:1763-1771.
29. Dai MS, Lu H. Inhibition of MDM2-mediated p53 ubiquitination and degradation by ribosomal protein L5. *J Biol Chem*. 2004;279:44475-44482.
30. Zhang Y, Wolf GW, Bhat K, et al. Ribosomal protein L11 negatively regulates oncoprotein MDM2 and mediates a p53-dependent ribosomal-stress checkpoint pathway. *Mol Cell Biol*. 2003;23:8902-8912.
31. Rao KC, Palamalai V, Dunlevy JR, et al. Peptidyl-Lys metalloendopeptidase-catalyzed ^{18}O labeling for comparative proteomics: application to cytokine/lipolysaccharide-treated human retinal pigment epithelium cell line. *Mol Cell Proteomics*. 2005;4:1550-1557.
32. Chao C, Saito S, Kang J. p53 transcriptional activity is essential for p53-dependent apoptosis following DNA damage. *EMBO J*. 2000;19:4967-4975.
33. Bai F, Matsui T, Ohtani-Fujita N, et al. Promoter activation and following induction of the p21/WAF1 gene by flavone is involved in G1 phase arrest in A549 lung adenocarcinoma cells. *FEBS Lett*. 1998;437:61-64.
34. Nyunoya T, Powers LS, Yarovinsky TO. Hyperoxia induces macrophage cell cycle arrest by adhesion-dependent induction of p21Cip1 and activation of the retinoblastoma protein. *J Biol Chem*. 2003;278:36099-360106.
35. Ortego J, Escribano J, Coca-Prados M. Gene expression of protease and protease inhibitors in the human ciliary epithelium and ODM-2 cells. *Exp Eye Res*. 1997;65:289-299.

85. 緑内障の動物モデル (1)
—霊長類モデル，ラットモデル—

岩田　岳
独立行政法人国立病院機構東京医療センター
臨床研究センター(感覚器センター)
分子細胞生物学研究部門

緑内障研究において動物モデルの存在はきわめて重要である．現在はおもに霊長類に加えてラットやマウスなどの齧歯(げっし)類が利用されている．本セミナーでは緑内障で利用されている動物モデルについて，2回シリーズで紹介したい．

はじめに

動物モデルの利点は，隅角や視神経・網膜における変化を発症過程に沿って詳細に解析できること，さらに新薬の評価を行えることである．これまでにも複数の哺乳類やその他の種で動物モデルの探索や開発が行われてきた[1]．利用目的に応じて1)ヒトとの視覚形態の類似性，2)発症までの時間，3)遺伝子操作の可能性，4)モデル動物作製に必要な技術，5)眼球の大きさ，6)解析に必要な技術，7)モデル動物の有効性，8)動物の維持費用などの検討が必要である．これまでにも異なる種で自然発症した緑内障モデル動物が紹介されているが，一般的には手術的あるいは遺伝子改変によって作製されたモデル動物が利用されている．

㊀霊長類モデル

すべての動物モデルのなかで隅角や視神経乳頭の構造がヒトと最も類似する霊長類モデルが研究に適していることはいうまでもないことである．特に房水流出機構に関する研究においては貴重な存在である．しかし，1頭当たりの維持費用がマウスの約100倍かかることや，飼育・管理に高度な知識・技術が必要であることから，多くの研究では利用されていない．房水流路の遮断にはおもに線維柱帯の光凝固が利用される[2,3]．この手法によって手術後数日間で25～60 mmHgの眼圧上昇が期待できる．その他の手法としては前房内に赤血球[4]，ラテックス[5]，ポリアクリルアミドゲル[6]，ステロイド[7]を注入することによって眼圧上昇を促す方法が報告されているが，光凝固によって最も安定した眼圧上昇が得られている[8]．霊長類における眼圧上昇は視神経乳頭，網膜神経線維，網膜神経節細胞層に障害[9]をもたらし，ヒトと同様な病理学的所見が再現されることが確認されている．また，霊長類モデルを利用した，光凝固後30日における網膜内の遺伝子発現の研究も報告されており[10]，この情報は新しい治療薬の開発にも利用されている．

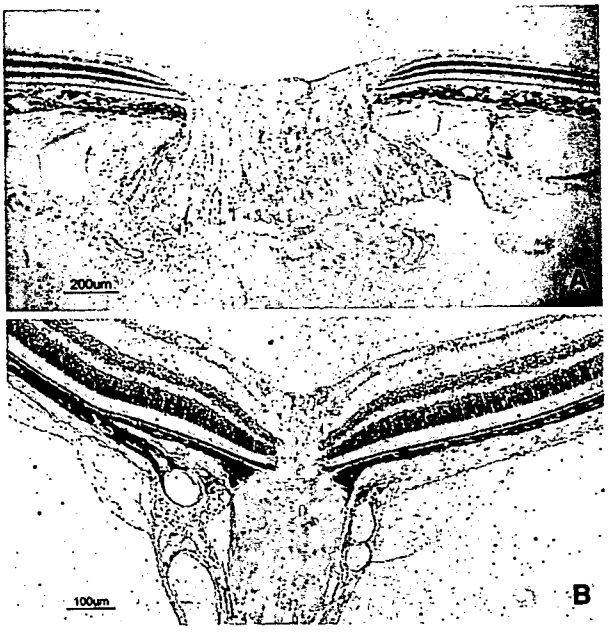

図1　カニクイザルとマウスの視神経乳頭の比較
カニクイザル(A)の視神経乳頭の構造はヒトときわめて類似しており，マウス(B)のそれとは大きく異なる．

㊁ラットモデル

動物モデルを用いて薬効評価を行う場合，実験には多数の動物が必要になる．このような場合にラットは有効である．ラットは簡単に飼育でき，性質もおとなしく，眼球も手ごろな大きさであることから，市販の機器を使って麻酔なしで眼圧測定ができる[11]．ラットの眼球には緑内障に関係する部位がすべて存在する．ラットにおける眼圧上昇は強膜静脈への生理食塩水の注入[12]，インドインクを使った線維柱帯の光凝固[13]，線維柱帯の光凝

0910-1810/07/¥100/頁/JCLS

固[14]，強膜静脈の焼灼[15]などの方法が用いられるが，研究者には高い技術が求められる．この方法によって最大約2倍眼圧上昇を急激に起こすことができる．眼圧上昇は通常数週間持続し，さらに2回目の光凝固が行われると，3週間以上の持続も可能である．眼圧上昇によってヒトに類似する網膜神経線維の萎縮や視神経乳頭の変化が観察できる[16,17]．ラットモデルの登場によって，眼圧上昇に伴う電気生理学的な研究や神経保護薬の開発，豊富な網膜の材料を使った遺伝子解析なども可能になった．眼圧が25～45 mmHgに上昇するRCS (Royal College of Surgeons) ラットも発見されており，網膜神経節細胞死や視神経乳頭陥凹などが観察されている．しかし残念ながらRCSラットにはチロシンキナーゼ遺伝子に変異があり，視細胞の変性が起こることから，緑内障モデルとしては敬遠されている．

次回は，マウスモデルとその他の動物モデルについて述べる．

文　献

1) Ritch R, Shields MB, Krupin T : Animal models of glaucoma. The Glaucomas (2nd ed), p55-69, Mosby-Year Book, St Louis, 1996
2) Gaasterland D, Kupfer C : Experimental glaucoma in the rhesus monkey. *Invest Ophthalmol Vis Sci* **13** : 455-457, 1974
3) Quigley HA, Hohman RM : Laser energy levels for trabecular meshwork damage in the primate eye. *Invest Ophthalmol Vis Sci* **24** : 1305-1307, 1983
4) Quigley HA, Addicks EM : Chronic experimental glaucoma in primates. I. Production of elevated intraocular pressure by anterior chamber injection of autologous ghost red blood cells. *Invest Ophthalmol Vis Sci* **19** : 126-136, 1980
5) Weber AJ, Zelenak D : Experimental glaucoma in the primate induced by latex microspheres. *J Neurosci Methods* **111** : 39-48, 2001
6) Kaufman PL, Lütjen-Drecoll E, Hubbard WC et al : Obstruction of aqueous humor outflow by cross-linked polyacrylamide microgels in bovine, monkey, and human eyes. *Ophthalmology* **101** : 1672-1679, 1994
7) Armaly MF : Aqueous outflow facility in monkeys and the effect of topical corticoids. *Invest Ophthalmol* **3** : 534-538, 1964
8) Rasmussen CA, Kaufman PL : Primate glaucoma models. *J Glaucoma* **14** : 311-314, 2005
9) Quigley HA, Nickells RW, Kerrigan LA et al : Retinal ganglion cell death in experimental glaucoma and after axotomy occurs by apoptosis. *Invest Ophthalmol Vis Sci* **36** : 774-786, 1995
10) Miyahara T, Kikuchi T, Akimoto M et al : Gene microarray analysis of experimental glaucomatous retina from cynomologous monkey. *Invest Ophthalmol Vis Sci* **44** : 4347-4356, 2003
11) Moore CG, Milne ST, Morrison JC : Noninvasive measurement of rat intraocular pressure with the Tono-Pen. *Invest Ophthalmol Vis Sci* **34** : 363-369, 1993
12) Morrison JC, Moore CG, Deppmeier LM et al : A rat model of chronic pressure-induced optic nerve damage. *Exp Eye Res* **64** : 85-96, 1997
13) Ueda J, Sawaguchi S, Hanyu T et al : Experimental glaucoma model in the rat induced by laser trabecular photocoagulation after an intracameral injection of India ink. *Jpn J Ophthalmol* **42** : 337-344, 1998
14) Levkovitch-Verbin H, Quigley HA, Martin KR et al : Translimbal laser photocoagulation to the trabecular meshwork as a model of glaucoma in rats. *Invest Ophthalmol Vis Sci* **43** : 402-410, 2002
15) Shareef SR, Garcia-Valenzuela E, Salierno A et al : Chronic ocular hypertension following episcleral venous occlusion in rats [letter]. *Exp Eye Res* **61** : 379-382, 1995
16) Garcia-Valenzuela E, Shareef S, Walsh J et al : Programmed cell death of retinal ganglion cells during experimental glaucoma. *Exp Eye Res* **61** : 33-44, 1995
17) Johnson EC, Morrison JC, Farrell S et al : The effect of chronically elevated intraocular pressure on the rat optic nerve head extracellular matrix. *Exp Eye Res* **62** : 663-674, 1996

☆　☆　☆

86. 緑内障の動物モデル (2)
—マウスモデル，その他—

岩田 岳
独立行政法人国立病院機構東京医療センター
臨床研究センター(感覚器センター)
分子細胞生物学研究部門

緑内障研究において動物モデルの存在はきわめて重要である．前号では霊長類とラットモデルについて紹介したが，今回はヒトにつぐ情報量と最新の遺伝子改変技術が利用できるマウスモデルについて，その眼球サイズが小さいことから生まれる実験のむずかしさを含めて紹介したい．

はじめに

霊長類や齧歯類モデルによってこれまでに緑内障の発症機序に関する貴重な情報が得られている．しかし，ヒトとの比較において，厳密には眼球の構造も異なっており，病気の進行速度も加速化されている場合もある．ここで紹介する各モデル動物で観察される現象はそのままヒトに当てはまるわけではない．しかし一つひとつの動物モデルは緑内障の一面を捉えていると考えられ，これらの情報を総合的に検討することによって，緑内障に関係する共通なメカニズムの発見につながる可能性がある．この点について，単一あるいは複数の遺伝子についてこれを欠損や過剰発現させる技術が確立しているマウスモデルには期待が寄せられている．

◎マウスモデル

マウスモデルはラットモデルの影で開発が遅れていたが，近年目覚しいマウスの遺伝子改変技術の進歩によって，目的とするトランスジェニックマウス，ノックアウトマウス，ノックインマウスなどが容易に作製されるようになり，眼球が小型であるという欠点がありながら，モデル動物として利用される機会が増加している．また，マウスは他の哺乳類に比べてデータベースが整備されており，遺伝子，蛋白質，代謝系，行動パターンに至るまで詳細な情報を手に入れることが可能である．

しかしながら，マウスには緑内障モデルとしての欠点も存在する．マウスとヒトでは視神経乳頭周辺の血管構造が異なることや，篩状板が存在しないなどの違いがあり[1]，眼球の取り扱いについても不利な面がある．その一つに眼圧測定のむずかしさがある．これまでにマウス専用の侵襲式や非侵襲式の眼圧測定法が開発されているが，最も信頼性の高い眼圧測定法としては，角膜の厚さや曲率半径などに影響されない侵襲式の方法がある．圧力計に接続したガラス管の針をマウスの前房に差し込み，眼圧を測定する方法である．この方法によって，異なるマウスの系について10～20 mmHgの眼圧差が存在することが明らかになった[2]．非侵襲式の利点は多数のマウスの眼圧を短い時間で測定できることであるが，角膜の性状に影響される．いずれの方法についても安定した結果を得るにはやはり訓練が必要である．

最近の遺伝子解析研究によってミオシリン，チトクローム *P4501B1*，オプチニュリン，*WDR36* が緑内障遺伝子として発見されているが，これらの遺伝子改変マウス

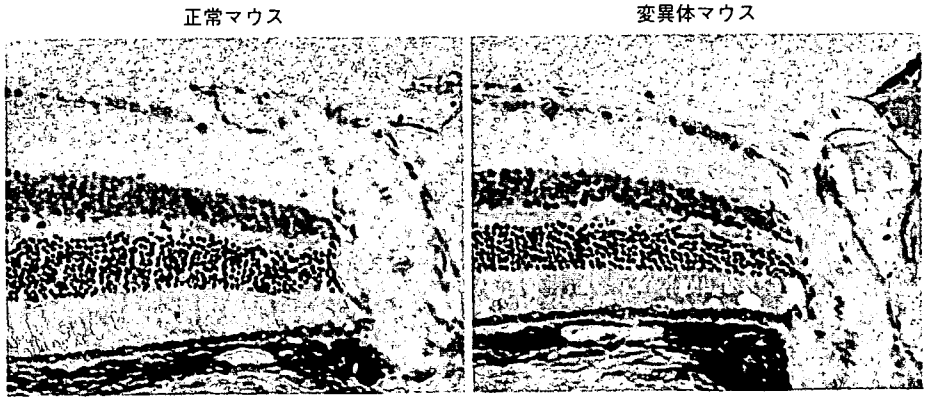

図1 正常マウスとオプチニュリン変異体(Glu50Lys)を発現するトランスジェニックマウスの視神経乳頭
変異体マウスでは網膜神経線維層が菲薄化している．

0910-1810/07/¥100/頁/JCLS

が緑内障を発症するのか研究が行われている．遺伝子改変マウスの利点は発症原因が明確なこと，手術的な方法に比べて表現型が安定していること，そして特別な訓練を必要とせずにネズミ算式に繁殖できることである．すでに複数の緑内障マウスが作製されているが，その一つにミオシリンのTyr437His変異を発現するトランスジェニックマウスがある．このマウスは正常マウスに比べて昼は2 mmHg，夜は4 mmHgの眼圧上昇が認められ，生後1年目には網膜神経節細胞数の20%が減少する[3]．コラーゲンタイプⅠα1サブユニットに遺伝子変異のあるトランスジェニックマウスではコラーゲンのメタロプロテアーゼ(MMP1)による分解が阻害され，生後36週ほどかけて眼圧が4.8 mmHg上昇することが報告されている．隅角の構造は保持されたまま，網膜神経節細胞層への障害が観察され，開放隅角緑内障マウスモデルとして認識されている[4]．また，筆者らはオプチニュリンGlu50Lys変異体を高発現したマウスを作製したところ，正常眼圧は維持されたまま，生後1年後には網膜神経節細胞死や視神経乳頭の陥凹が観察されている．

マウスに対する手術的な眼圧上昇はラットよりもさらに困難である．C57BL/6Jマウスの前房にインドシアニングリーンを注入し，線維柱帯と上強膜静脈部位の光凝固を施すと，約10日後に眼圧が正常なマウスの15.2±0.6 mmHgに対して33.6±1.5 mmHgに上昇したが，60日後には正常値に戻ったと報告されている[5]．網膜神経節細胞層や網膜への機能障害がERG(網膜電図)などによって明らかにされている．Simon Johnらによって報告されたDBA/2Jマウスは2つの遺伝子*Tyrp1*と*Gpnmb*[6]に変異があり，色素顆粒の分散による虹彩の萎縮が起こり，虹彩癒着によって生後9カ月後には眼圧が上昇し，視神経乳頭を基点として網膜神経節細胞死が扇状に観察されている[7]．

❹その他の動物モデル

その他の動物モデルにはウサギ，ブタ，ウシなどが報告されているが，広く利用されていない．眼における遺伝子の機能をすばやくおおざっぱに調べる方法として，ゼブラフィッシュ(zebrafish)を利用した研究が最近報告されており，ミオシリン，オプチニュリン，*WDR36*などの欠損による眼球への影響が報告されている[8]．残念ながら眼圧は測定できない．

文　献

1) May CA, Lutjen-Drecoll E : Morphology of the murine optic nerve. *Invest Ophthalmol Vis Sci* **43** : 2206-2212, 2002
2) Savinova OV, Sugiyama F, Martin JE et al : Intraocular pressure in genetically distinct mice : an update and strain survey. *BMC Genet* **2** : 12, 2001
3) Senatorov VV, Malyukova I, Fariss R et al : Expression of mutated mouse myocilin induces open-angle glaucoma in transgenic mice. *J Neurosci* **26** : 11903-11914, 2006
4) Mabuchi F, Lindsey JD, Aihara M et al : Optic nerve damage in mice with a targeted type I collagen mutation. *Invest Ophthalmol Vis Sci* **45** : 1841-1845, 2004
5) Grozdanic SD, Betts DM, Sakaguchi DS et al : Laser-induced mouse model of chronic ocular hypertension. *Invest Ophthalmol Vis Sci* **44** : 4337-4346, 2003
6) Anderson MG, Smith RS, Hawes NL et al : Mutations in genes encoding melanosomal proteins cause pigmentary glaucoma in DBA/2J mice. *Nat Genet* **30** : 81-85, 2002
7) Jakobs TC, Libby RT, Ben Y et al : Retinal ganglion cell degeneration is topological but not cell type specific in DBA/2J mice. *J Cell Biol* **171** : 313-325, 2005
8) McMahon C, Semina EV, Link BA : Using zebrafish to study the complex genetics of glaucoma. *Comp Biochem Physiol C Toxicol Pharmacol* **138** : 343-350, 2004

☆　☆　☆

難治性疾患克服研究事業

黄斑変性カニクイザルを用いた補体活性抑制剤による加齢黄斑変性の予防・治療法の確立と情報収集システムの開発

(H18 - 難治 - 一般 - 001)

平成１９年度　総括研究報告書

主任研究員　　岩田　岳

平成20年3月